

Formation of Chrysocolla and Secondary Copper Phosphates in the Highly Weathered Supergene Zones of Some Australian Deposits

MARTIN J. CRANE, JAMES L. SHARPE AND PETER A. WILLIAMS

School of Science, University of Western Sydney,
Locked Bag 1797, Penrith South DC NSW 1797, Australia
p.williams@uws.edu.au (corresponding author)

ABSTRACT. Intense weathering of copper orebodies in New South Wales and Queensland, Australia has produced an unusual suite of secondary copper minerals comprising chrysocolla, azurite, malachite and the phosphates libethenite and pseudomalachite. The phosphates persist in outcrop and show a marked zoning with libethenite confined to near-surface areas. Abundant chrysocolla is also found in these environments, but never replaces the two secondary phosphates or azurite. This leads to unusual assemblages of secondary copper minerals, that can, however, be explained by equilibrium models. Data from the literature are used to develop a comprehensive geochemical model that describes for the first time the origin and geochemical setting of this style of economically important mineralization.

CRANE, MARTIN J., JAMES L. SHARPE & PETER A. WILLIAMS, 2001. Formation of chrysocolla and secondary copper phosphates in the highly weathered supergene zones of some Australian deposits. *Records of the Australian Museum* 53(1): 49–56.

Recent exploitation of oxide copper resources in Australia has enabled us to examine supergene mineral distributions in several orebodies that have been subjected to intense weathering. These include deposits at Girilambone (Gilligan & Byrnes, 1994) and Goonumbla or Northparkes in NSW (Heithersay *et al.*, 1990; Crane *et al.*, 1998) and several smaller deposits in the Mt. Isa Block in northwest Queensland (Ball, 1908; Day & Beyer, 1995; Carter *et al.*, 1961). Consequences of the intense weathering of these deposits include the mobilization of silica and subsequent formation of considerable quantities of chrysocolla and secondary silica in the oxidized zones. Furthermore, all of

these deposits are characterized by an abundance of the secondary copper phosphates libethenite and pseudomalachite associated with smaller amounts of cornetite and turquoise.

Although the secondary mineral distributions in these deposits vary, a number of recurring paragenetic relationships are evident. The copper carbonates malachite and azurite are seldom replaced by chrysocolla, nor are the secondary copper phosphates. Chrysocolla and/or secondary silica frequently envelop copper carbonates and phosphates, the more stable phases in such environments. Characteristic zoning of the phosphate minerals has also been noted, with

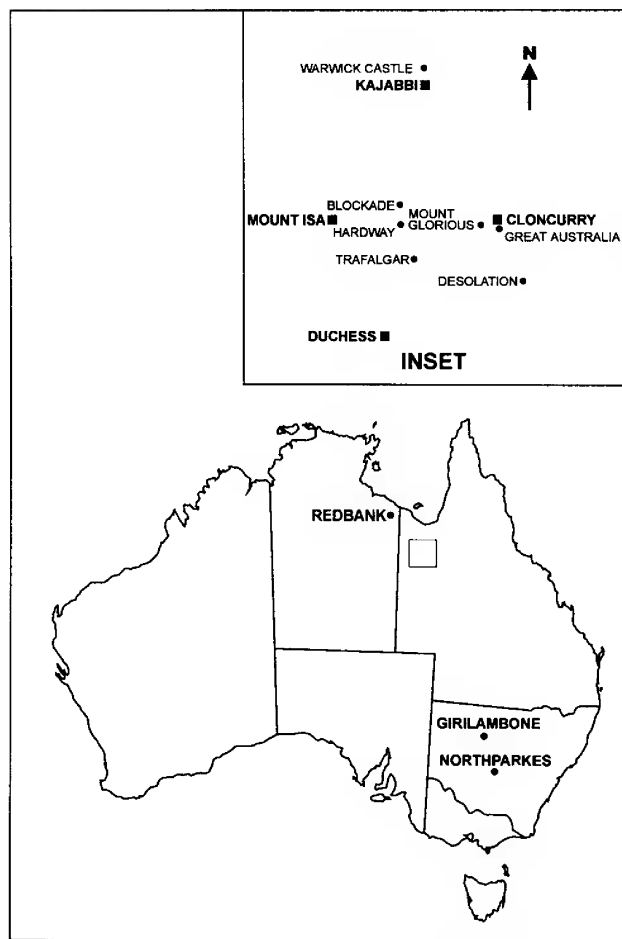


Figure 1. Locations of the deposits included in this study.

libethenite invariably being found nearer the surface. Repetition of these observations across a number of sites has prompted an investigation into the equilibrium chemistry of these minerals. An equilibrium approach was found to explain many of the parageneses noted, and the findings appear to be characteristic of the type of oxidized mineral zones involved. The locations of the deposits studied are shown in Figure 1.

Phosphate minerals

The distribution of secondary copper phosphates in the Northparkes orebodies has been described previously by Crane *et al.* (1998). Here libethenite $[\text{Cu}_2\text{PO}_4(\text{OH})]$ and pseudomalachite $[\text{Cu}_5(\text{PO}_4)_2(\text{OH})_4]$ are the dominant copper minerals at the base of extensively leached kaolinized zones and are associated with secondary silica, chrysocolla (*vide infra*) and malachite, $[\text{Cu}_2\text{CO}_3(\text{OH})_2]$. Particularly noteworthy are rhythmically banded, botryoidal malachite-pseudomalachite composites comprised of individual layers up to a few tenths of a millimetre thick. Similar material has been recovered from the upper sections of the Main Lode at the Great Australia mine, Cloncurry (Day & Beyer 1995) where, in the outcrop, the malachite had been leached

from the composites to leave shells of pseudomalachite (Fig. 2). Similar rhythmic banding involving the same minerals was noted in the upper sections of the oxidized zone of the Warwick Castle lode, north of Kajibbi.

With respect to replacement textures, pseudomorphs of pseudomalachite after azurite have been collected from the 10271 bench in the E27 deposit at Northparkes (Crane *et al.*, 1998). Other material shows pseudomalachite as a coating of crystal aggregates over azurite crystals and in some instances, the azurite has subsequently dissolved to yield pseudomalachite endomorphs.

A separate, but remarkable, observation in many of the deposits is the zoning of the secondary copper phosphates in the supergene profile. In particular, libethenite is always found near the top of the oxidized zone. At Northparkes, weathering of the host quartz monzonite porphyry has produced bleached, kaolinized zones from which all visible traces of copper mineralization have been removed (Crane *et al.*, 1998). Immediately beneath these zones, pseudomalachite and libethenite are associated with secondary manganese oxides. Libethenite is limited to the top contact of the oxidized zones with pseudomalachite persisting a few metres deeper and grading into more conventional malachite—azurite and then cuprite—native copper—chalcocite assemblages.

Kaolinization of host rocks at Girilambone and Great Australia, chlorite sericite schists and metadolerites, respectively, is of more limited extent than at Northparkes, and results from sulphuric acid generation as the result of the oxidation of pyrite. In both deposits, secondary copper phosphate mineralization was extensive.

Pseudomalachite and libethenite were present in the outcrop of the Great Australia Main Lode, with the former occurring abundantly as casts in friable goethite-hematite gossan. Libethenite was found near the surface, both in vughs in ferruginous quartz and also associated with pseudomalachite and cornetite, in vughs in altered tuffs. As mining of the oxide zone proceeded, abundant libethenite was found in and immediately beneath the silicified gossan of the Main Lode, particularly towards the northern end of the main open cut. Aggregates of acicular and etched crystals to 10 mm were scattered over joints and fractures and in vughs in ferruginous lode quartz and in silicified gossan, sometimes accompanied by turquoise. However, all traces of libethenite had vanished at a depth of about 15 m. Pseudomalachite, occurring as crystal aggregates or bunches coating vughs in friable gossan and as banded botryoidal material associated with malachite, persisted to the base of bench 11 (c. 35 m from surface) in the Main Lode. Little phosphate mineralization was noted in the intersecting B Tangye Lode.

At Girilambone, coarsely crystallized libethenite (as prisms to 2.5 cm) was confined to a zone extending from 10 to 18 m from the surface, particularly in friable quartzite gossan. Occasional spherules and coatings of turquoise were present in this material. In contrast, pseudomalachite was a comparatively common secondary phase in the main pit at Girilambone and extended through the libethenite zone to Bench 28, approximately 90 m from the surface. It principally occurred in or near the quartzite gossan as crystal



Figure 2. Pseudomalachite casts; Main Lode outcrop, Great Australia mine, Cloncurry, Queensland. The field of view is c. 8 cm across.

aggregates and bunches and as occasional stalactites mixed with malachite. Often, single crystals of azurite were embedded in the pseudomalachite; azurite was always a frequent associate.

In other copper deposits in the Mt. Isa Block, the same zoning is evident. At Warwick Castle, libethenite as acicular and platy crystals to 8 mm liberally coated shattered lode quartz and joints in altered metabasalts in the lode outcrop, associated with minor pseudomalachite and chrysocolla. Libethenite was confined to a near surface (<10 m) zone, with pseudomalachite, occurring as crystal clots and rhythmically banded aggregates with malachite, persisting deeper than 30 m (190 RL bench). Here it was also present as coatings of crystal aggregates on quartz-rich gossan associated with chrysocolla and azurite. Similarly, multiple generations of libethenite and pseudomalachite were confined to the top-most sections of the Sandy Flat pipe at Redbank, Northern Territory, at the northwest extremity of the Mt. Isa Block (McLaughlin *et al.*, 2000). At the Hardway mine, near Mt. Isa, libethenite associated with pseudomalachite occurs in a kaolinized quartz-rich gossan at the surface and persisting to a depth of a few metres in a small open cut. At the Desolation prospect, south of Cloncurry, libethenite and pseudomalachite occur in small pits within a metre of the surface, associated with malachite, chrysocolla and the secondary arsenates olivenite [$\text{Cu}_2\text{AsO}_4(\text{OH})$], conichalcite [$\text{CaCuAsO}_4(\text{OH})$], and clinoclase [$\text{Cu}_3\text{AsO}_4(\text{OH})_3$], these arsenates being the result of oxidation of arsenopyrite, cobaltite and chalcopyrite.

Chemical relationships of the phosphate minerals

Thermodynamic data for libethenite, pseudomalachite and cornetite [$\text{Cu}_3\text{PO}_4(\text{OH})_3$] and the equilibrium relationships of these minerals with malachite and azurite [$\text{Cu}_3(\text{CO}_3)_2(\text{OH})_2$] (Magalhães *et al.*, 1986, 1988), show that, in general, equilibrium paths between the copper phosphates and the carbonates are restricted. Thus, whilst routes are available for pseudomalachite and cornetite to azurite transformations, and for cornetite to malachite transformations, malachite and pseudomalachite cannot directly replace each other, because of thermodynamic constraints, under normal supergene conditions. Intermediate steps involving azurite or cornetite are necessary, thus making malachite-pseudomalachite assemblages quite stable under conditions in which appropriate kinetic factors operate.

This appears to be the case with the deposits mentioned above in that the rhythmically banded malachite—pseudomalachite simply reflects the fluctuating availability of $\text{H}_2\text{PO}_4^{2-}(\text{aq})$ or $\text{HPO}_4^{2-}(\text{aq})$ versus $\text{HCO}_3^{-}(\text{aq})$ or $\text{CO}_3^{2-}(\text{aq})$ in mineralizing solutions. When more phosphate was present, pseudomalachite would form because of its lower solubility (although perhaps *via* a thin and subsequently pseudomorphed layer of cornetite). Weathering of malachite-pseudomalachite aggregates to leave pseudomalachite as thin casts probably represents the result of similar solubility differences to those mentioned above, as well as to the fact that pseudomalachite dissolves reversibly

in weakly acid solutions much more slowly than does malachite, the latter involving loss of $\text{CO}_2(\text{g})$.

The rare occurrence of cornetite, confined to the Great Australian Main Lode outcrop (Day & Beyer 1995) in the deposits examined, is due to its formation under somewhat more unusual chemical conditions (relatively higher pH, higher copper and lower phosphate ion activities) compared to those responsible for the crystallization of pseudomalachite and libethenite (Magalhães *et al.*, 1986, 1988). Considerable variation in these parameters at the Great Australia deposit is evidenced by the presence of all possible parageneses of these minerals in the outcrop of the Main Lode. Reference to the equilibrium pH-activity diagram in Figure 3 (Magalhães *et al.*, 1986, 1988) suggests that the occurrence of cornetite at this locality may be related to higher pH regimes, since the outcrop occurs in the vicinity of carbonate rocks of the Corella Formation.

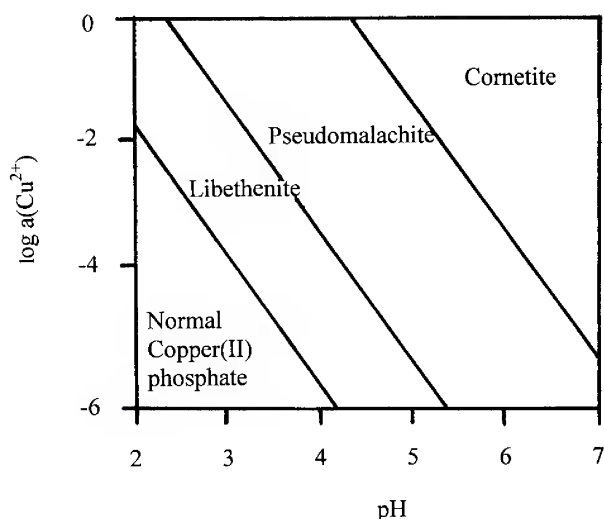


Figure 3. Equilibrium pH- Cu^{2+} activity diagram showing stability fields of the secondary copper phosphates at 25°C. Boundary conditions refer to equations written so that dihydrogen phosphate ion activity is not a variable.

Field observations above support the conclusion that libethenite typically occurs in the upper part of the oxidized zone, with pseudomalachite forming further down. The reason for this is not readily apparent from an inspection of equilibrium relations (Fig. 3), although it does explain the rarity of cornetite by fact that it can only form under comparatively basic conditions. However, the equilibrium relations can be recast in such a way that the observed zoning is easily understood, as shown in Figure 4. Here the constraints of pH are such that $\text{H}_2\text{PO}_4^-(\text{aq})$ is the predominant phosphate species in solution. These relations now indicate that libethenite forms at the most concentrated phosphate activities, while pseudomalachite forms from solutions with lower amounts of dissolved phosphate. It is thus appropriate that the phosphate source be considered.

In a classical study of the weathering of a gneiss, Goldich (1938) found that apatite, the most probable source of phosphate for all the above species, was among the least

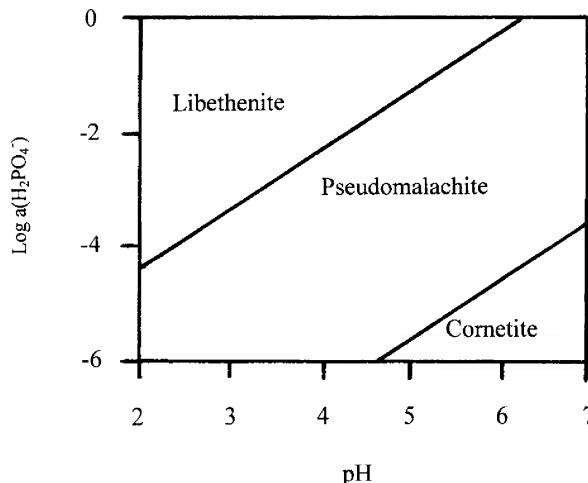
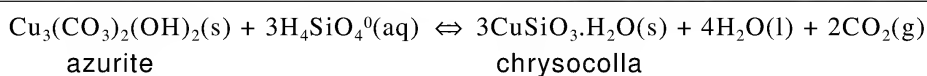


Figure 4. Equilibrium pH- $\text{H}_2\text{PO}_4^{2-}$ diagram for the secondary copper phosphate minerals at 25°C. Boundary conditions refer to equations written so that copper ion activity is not a variable.

stable minerals. Ollier (1984) noted that, of the apatite group, hydroxylapatite was most easily weathered and chloroapatite less so, while fluorapatite is somewhat more resistant to weathering. Thus the observed zoning of the copper phosphate minerals may simply be accounted for by the local phosphate distribution, related to variations in the intensity of weathering of the host rocks. The most intense weathering is usually at the surface and will lead to higher phosphate concentrations in downward-percolating groundwater, thus making the formation of libethenite more likely near the surface. As weathering intensity diminishes with depth, less phosphate will be available and pseudomalachite will dominate the secondary copper phosphates. This model, together with appropriate pH control, serves to unify all of the occurrences of the secondary copper phosphates in the deposits we have examined. Finally in this regard, Stumm & Morgan (1981) suggest that the formation of hydroxylapatite controls phosphate concentrations in groundwaters. At Northparkes, secondary hydroxylapatite is one of the last minerals to form in the oxidized zone and is commonly found as hexagonal plates to 1 mm on pseudomalachite and chrysocolla endomorphs after libethenite. No copper minerals were observed to form after hydroxylapatite (Crane *et al.*, 1998), suggesting depletion of copper with extended leaching.

Chrysocolla

Chrysocolla is a secondary copper silicate, which occurs abundantly in oxidized copper orebodies worldwide (Roberts *et al.*, 1990). However, its structure is poorly characterized as a result of its invariably quasi-amorphous nature. Van Oosterwyck-Gastuche & Grégoire (1971) proposed a chain structure for fibrous microcrystals from 0.5 to 3 microns long and 60–70 nm across, which corresponds with an idealized formula of $\text{Cu}_2\text{H}_2(\text{Si}_2\text{O}_5)(\text{OH})_4 \cdot n\text{H}_2\text{O}$. This formulation is supported by the work of Chukrov *et al.* (1968) and a number of analyses of chrysocolla containing



small amounts of other metals such as Al^{3+} substituting for Cu^{2+} , with charge compensation for Al^{3+} being maintained by variation of the number of protons present (Van Oosterwyck-Gastuche, 1970; Kiseleva *et al.*, 1991).

Chrysocolla specimens examined from the deposits discussed here and elsewhere give more or less broad reflections in X-ray powder diffraction (XRD) patterns, indicating variable degrees of order; all are cryptocrystalline and grade into copper-stained amorphous silica and quartz from sample to sample. At Great Australia, chrysocolla in the upper levels of the B Tangye Lode is more crystalline than chrysocolla encountered elsewhere, except for the Trafalgar deposit, south of Cloncurry (Fig. 1), and is comparatively ordered, as judged from the XRD pattern.

The end-member formula above is based on structural information but may be reduced to $\text{CuH}_2\text{SiO}_4 \cdot n\text{H}_2\text{O}$ or $\text{CuSiO}_3 \cdot n\text{H}_2\text{O}$, as has been written in the older literature. Newberg (1967) defined a partially dehydrated chrysocolla and gave its formula as $\text{CuSiO}_3 \cdot \text{H}_2\text{O}$. This formulation was used in his experiments to determine the thermodynamic properties of chrysocolla from solubility measurements. A value of the standard Gibbs free energy of formation, $\Delta_f G^\circ$, for amorphous chrysocolla was calculated as $-1206.7 \text{ kJ mol}^{-1}$ and $-1218.4 \text{ kJ mol}^{-1}$ for diopside as an "aged" chrysocolla precipitate, at 298.2K. Diopside, while it can be assigned a reduced stoichiometry of $\text{CuSiO}_3 \cdot \text{H}_2\text{O}$ as well, is however a crystalline monocyclosilicate of ring periodicity six. Its structure is well established by single-crystal X-ray studies (Ribbe *et al.*, 1977; Belov *et al.*, 1978). More recently, an accurate value for $\Delta_f G^\circ$ (diopside, s, 298.2K) has been reported (Kiseleva *et al.*, 1993) and a value of $-1220.8 \pm 4.6 \text{ kJ mol}^{-1}$ was derived *via* calorimetric measurements for the formula $\text{CuSiO}_3 \cdot \text{H}_2\text{O}$. The comparative rarity of diopside versus chrysocolla, must then be based on kinetic factors related to the ease and frequency of formation of appreciable amounts of the cyclic $\text{H}_{12}\text{Si}_6\text{O}_{18}$ polymer or its conjugate anions in solutions of silicic acid at low temperatures. Thus it is reasonable to take the more negative value of Newberg (1967) given above to represent cryptocrystalline chrysocolla. We have used this value in our calculations, which have proved to provide an explanation for many observations involving chrysocolla's paragenetic relationships.

The limits of concentration of dissolved silica in aqueous solutions at 25°C have been reviewed by many workers (Iler 1979; Stumm & Morgan 1981; Dove 1995) and continue to attract attention as new silica polymorphs are identified (Gislason *et al.*, 1997). At 298.2K and 10^5 Pa , amorphous silica reaches an equilibrium concentration in water of $10^{-2.71} \text{ mol dm}^{-3}$ at neutral values of pH (solubility increases in basic solution as the contributions of conjugate anions of silicic acid become more important). For our considerations below, we have chosen this value to represent the maximum activity of silicic acid in water under these conditions; in thermodynamic terms, this is acceptable for calculations even though it is known that dimers are present as well (Dove 1995; Applin 1987).

Known relationships between the secondary copper carbonates and chrysocolla are comparatively simple, and have widespread application to observations of natural assemblages. First, at CO_2 pressures sufficiently high to make azurite stable with respect to malachite (c. $10^{-1.35}$; Williams, 1990), chrysocolla cannot replace azurite. Hence, for the equation shown above, at or above the given pressure, there is no achievable activity of $\text{H}_4\text{SiO}_4^0(\text{aq})$ such that azurite becomes unstable with respect to chrysocolla. Thus the remarkable examples of chrysocolla coating azurite at Northparkes (Crane *et al.*, 1998) appear to have formed simply by the later crystallization of chrysocolla on pre-existing azurite. Similar assemblages are found in the Queensland deposits mentioned previously, where azurite occurs near the surface.

However, mention should be made of reports of chrysocolla pseudomorphs after azurite and malachite (see, for example, Thompson 1980; Bywater 1984). Such observations are readily explained by reference to Figure 5 which shows that while azurite cannot be directly transformed to chrysocolla, malachite can be, and other conditions exist such that chrysocolla can only form coatings on pre-existing malachite. Thus, reported chrysocolla pseudomorphs after malachite are seen as arising simply from the existence of the appropriate chemical conditions, whereas reported chrysocolla pseudomorphs after azurite are in fact chrysocolla *after malachite* after azurite. Many specimens showing the formation of secondary silica and chrysocolla (especially in the upper sections of oxidized zones in the Mt. Isa Block) are known, the intense silicification of these bodies being directly related to the high degree of weathering of the enclosing rocks.

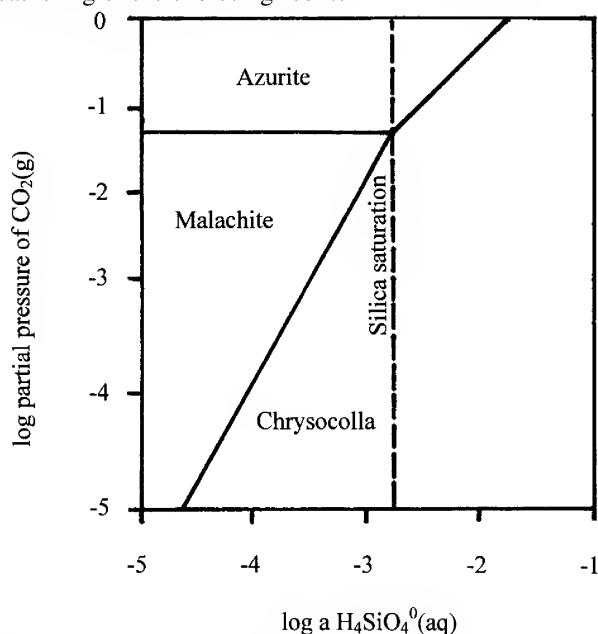


Figure 5. Stability fields for chrysocolla *versus* malachite and azurite at 25°C. The dashed line represents the limit of silicic acid activity in equilibrium with amorphous silica.

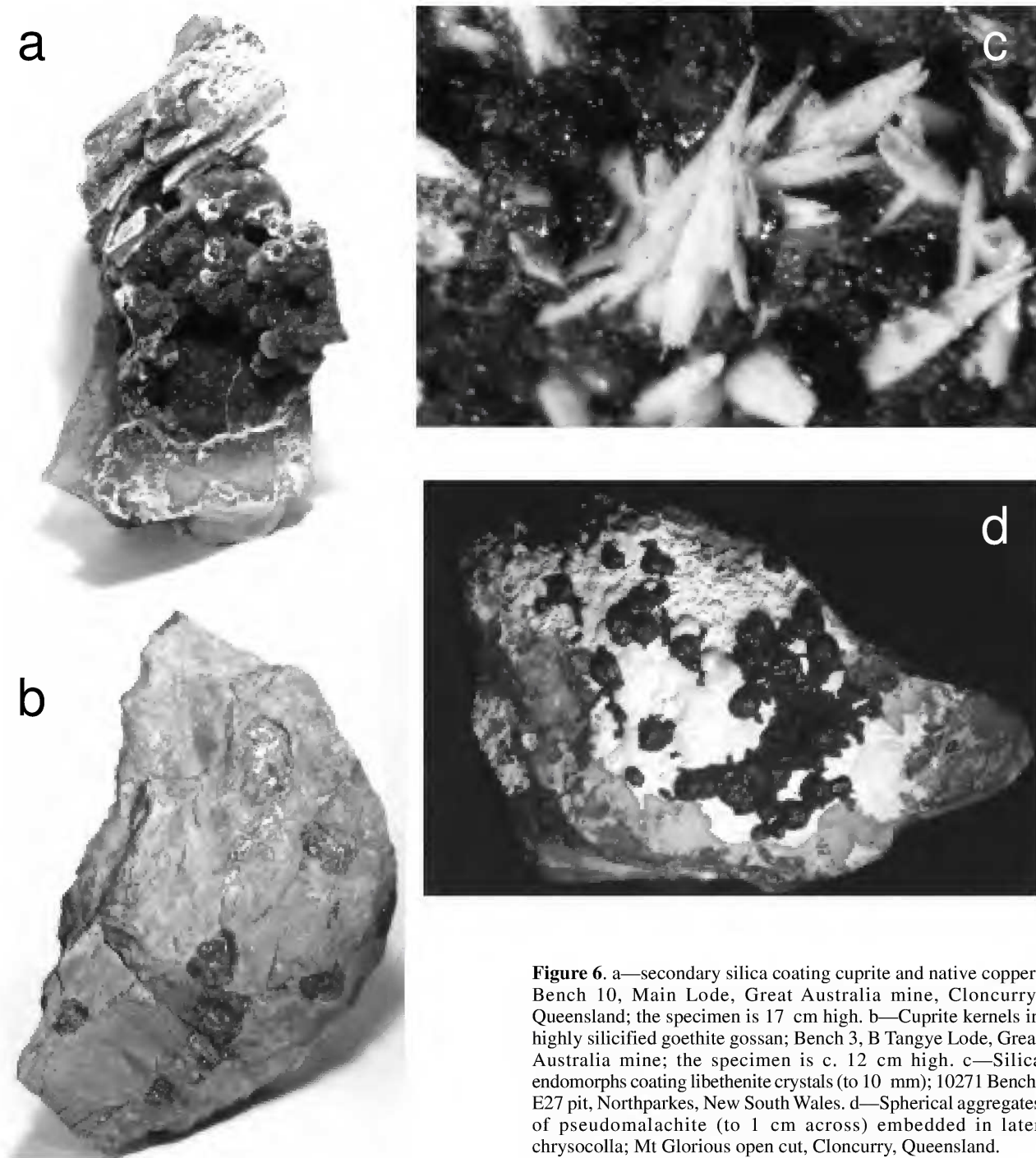


Figure 6. a—secondary silica coating cuprite and native copper; Bench 10, Main Lode, Great Australia mine, Cloncurry, Queensland; the specimen is 17 cm high. b—Cuprite kernels in highly silicified goethite gossan; Bench 3, B Tangye Lode, Great Australia mine; the specimen is c. 12 cm high. c—Silica endomorphs coating libethenite crystals (to 10 mm); 10271 Bench, E27 pit, Northparkes, New South Wales. d—Spherical aggregates of pseudomalachite (to 1 cm across) embedded in later chrysocolla; Mt Glorious open cut, Cloncurry, Queensland.

At the Great Australia mine, abundant secondary quartz, chalcedony and chrysocolla occur throughout the oxidized zone of the Main and B Tangye Lodes. In the former, secondary quartz completely enclosing otherwise unaltered malachite, cuprite and native copper crystals was common at depths below 20 m (Fig. 6a) and a completely silicified goethitic gossan was a feature of upper levels of the B Tangye Lode (Fig. 6b). Secondary silica infiltration of this section of the deposit gave a characteristic brown, cherty material studded with

kernels of native copper and cuprite, and occasional chalcocite and digenite, which had been rendered impervious to subsequent attack by aqueous solutions and persisted to within 10 m of the surface

Chrysocolla-coated malachite has been recovered from the Trafalgar, Warwick Castle, Desolation and Mt. Glorious deposits, and mines grouped around the Blockade mine, near Mt. Isa. Chrysocolla pseudomorphs after malachite are present in these deposits as well, especially at the Trafalgar mine.

Relationships between the secondary copper phosphates and chrysocolla are similar to the above in some respects, but more complex. Figure 7 shows equilibrium conditions calculated by the authors for these species, for pH values between 3 and 7, where $\text{H}_4\text{SiO}_4^0(\text{aq})$ and $\text{H}_2\text{PO}_4^-(\text{aq})$ are the dominant dissolved silica and phosphate species, respectively. Reference to this figure leads to a remarkable conclusion. There is no achievable $\text{H}_4\text{SiO}_4^0(\text{aq})$ activity when libethenite is the thermodynamically stable secondary copper phosphate, such that chrysocolla can replace libethenite. It must form together with it, when silica concentrations exceed saturation. Thus the phosphate-silicate assemblages from the upper levels of the Northparkes oxidized zones are explained. Silica and chrysocolla coat, but do not replace, libethenite (Fig. 6c). Subsequent dissolution of libethenite with changing solution chemistry has led to the preservation of chrysocolla and secondary silica endomorphs, as also seen in Figure 6. Again using Figure 7, the same explanation can be applied to the occurrence of chrysocolla and secondary silica on pseudomalachite, although saturated solutions of silicic acid do approach values which would lead to chemical attack. Phosphate values must fall to levels consistent with the stability of cornetite for chrysocolla to directly replace the copper phosphates. Abundant crystalline libethenite in the outcrop at the Hardway and Warwick Castle deposits further attest to the stability of libethenite over chrysocolla under all naturally achievable chemical conditions.

Many examples of the preservation of pseudomalachite in highly silicified secondary copper ores have been encountered. For example, it forms radiating crystal aggregates to 1 cm embedded in chrysocolla at Mt. Glorious (Fig. 6d). Chrysocolla and chalcedony coat and embed both pseudomalachite and libethenite in the Main Lode at the Great Australia Mine, and commonly in the Redbank and Trafalgar deposits.

Other relationships observed in the field can be attributed to kinetic factors. Rhythmically banded pseudomalachite–chrysocolla crusts from Northparkes are seen as arising from silica interaction with previously mentioned pseudomalachite–malachite assemblages (i.e., replacement of malachite by chrysocolla). The failure to observe pseudomalachite–cornetite transitions can be attributed to the preservation of chemical conditions such that pseudomalachite remains stable, coupled with the fact that compact crusts of pseudomalachite are rather slow to dissolve in aqueous solutions at room temperature (M.J. Crane and P.A. Williams, unpublished results). The preservation of pseudomalachite in the upper sections of oxidized ores of the Mt. Isa Block, particularly at Mt. Glorious and Great Australia is also due to this kinetic influence.

Conclusions

Sometimes unexpected assemblages of secondary copper phosphates with malachite, azurite and chrysocolla in highly weathered terrains can be explained using simple equilibrium models for mineral formation. Such models have been successfully applied to deposits at Girilambone

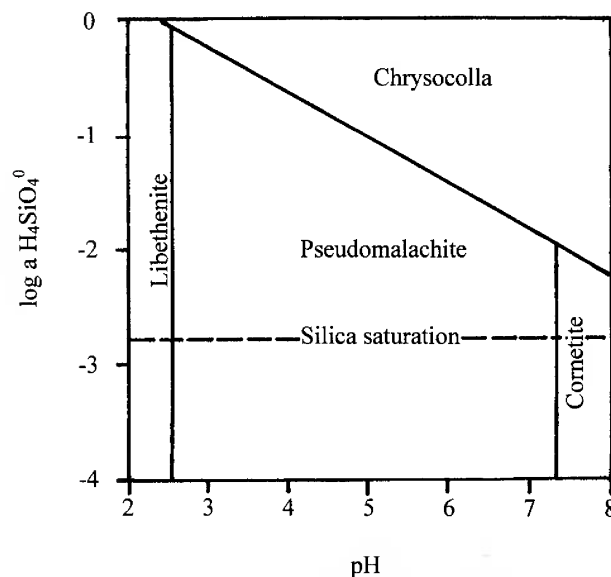


Figure 7. Stability field diagram for the secondary copper phosphates *versus* chrysocolla at 25°C. The dashed line represents the limit of silicic acid activity in equilibrium with amorphous silica.

and Northparkes, NSW, and to numerous oxidized copper lodes in the Mt. Isa Block, Queensland. The persistence of libethenite and pseudomalachite in these deposits is due to their particular chemical stabilities, which can be used to explain the development of pseudomorphous replacements of various kinds, especially those involving chrysocolla. For the first time, a comprehensive explanation of the chemical conditions responsible for the formation of this style of economically important mineralization has been provided.

ACKNOWLEDGMENTS. We wish to acknowledge the assistance of the staff of the Girilambone Copper Company, North Limited, Majestic Resources, Murchison United and Cloncurry Mining, and for permission to carry out research on their properties. Special thanks are due to Brett Tulloch and Jim and Annette Heape of Cloncurry Mining for help with fieldwork and the location of obscure mines and prospects. We also acknowledge the suggested improvements to the manuscript of two referees; these have considerably strengthened the paper.

References

- Applin, K.R., 1987. The diffusion of dissolved silica in dilute aqueous solution. *Geochimica et Cosmochimica Acta* 51: 2147–2151.
- Ball, L.C., 1908. Cloncurry Copper Mining District. Part 2. *Queensland Geological Survey Publication*, no. 215.
- Belov, N.V., B.A. Maksimov, Y.Z. Nozik & L.A. Muradyan, 1978. Refining the crystal structure of diopside $\text{Cu}_6[\text{Si}_6\text{O}_{18}]\cdot 6\text{H}_2\text{O}$ by X-ray and neutron-diffraction methods. *Soviet Physics Doklady* 23: 215–217.
- Bywater, S.K.G., 1984. Pseudomorphs from the Burra mine, South Australia. *Mineralogical Record* 15: 105–108.

- Carter, E.K., J.H. Brooks & K.R. Walker, 1961. The Precambrian belt of north-western Queensland. *Australian Bureau of Mineral Resources Bulletin*, no. 51.
- Chukrov, F.V., G. Zviagin, A.J. Gorshkov, L.P. Yermilova & Y.S. Rudnitskaya, 1968. Chrysocollas. *International Geology Survey* 11: 570–581.
- Crane, M.J., J.L. Sharpe & P.A. Williams, 1998. The mineralogy of the oxidized zones of the E22 and E27 orebodies at Northparkes, NSW. *Australian Journal of Mineralogy* 4: 3–8.
- Day, B.E., & B. Beyer, 1995. Some mines of the Mt. Isa district. Part 1. The Great Australia Mine. *Australian Journal of Mineralogy* 1: 23–28.
- Dove, P.M., 1995. Kinetic and thermodynamic controls on silica reactivity in weathering environments. In *Chemical Weathering Rates of Silicate Minerals*, eds. A.F. White & S.L. Brantley, *Reviews in Mineralogy* 31: 235–290. Washington: Mineralogical Society of America.
- Gilligan, L.B., & J.G. Byrnes, 1994. *Metallogenic Study and Mineral Deposit Data Sheets: Cobar 1:250000 Metallogenic Map SH/55-14*. Sydney: New South Wales Department of Mineral Resources.
- Gisslasson, S.R., P.J. Heaney, E.H. Delkers & J. Schott, 1997. Kinetic and thermodynamic properties of moganite, a novel silica polymorph. *Geochimica et Cosmochimica Acta* 61: 1193–1204.
- Goldich, S.S., 1938. A study of rock weathering. *Journal of Geology* 46: 17–58.
- Heithersay, P.S., W.J. O'Neill, P. van der Helder, C.R. Moore & P.G. Harbon, 1990. Goonumbla Porphyry Copper District—Endeavour 26 North, Endeavour 22 and Endeavour 27 copper gold deposits. In *Geology of the Mineral Deposits of Australia and Papua New Guinea*, ed. F.E. Hughes, pp. 1385–1398. Melbourne: Australasian Institute of Mining and Metallurgy.
- Iler, R., 1979. *The Chemistry of Silica*. New York: Wiley & Sons.
- Kiseleva, I.A., L.P. Ogorodova, L.V. Melchakova, M.R. Bisengalieva & N.S. Bekturganov, 1991. Thermodynamic properties of chrysocolla. *Transactions of the University of Moscow, Series 4: Geology* 1: 55–64 [*Chemical Abstracts* 115: 283672 (1991)].
- Kiseleva, I.A., L.P. Ogorodova, L.V. Melchakova & M.R. Bisengalieva, 1993. Thermodynamic properties of copper silicate: diopside: $\text{Cu}_6\text{Si}_6\text{O}_{18} \cdot 6\text{H}_2\text{O}$. *Journal of Chemical Thermodynamics* 25: 621–630.
- Magalhães, M.C.F., J.D. Pedrosa de Jesus & P.A. Williams, 1986. Stability constraints and formation of Cu(II) and Zn(II) phosphate minerals in the oxidized zone of base metal orebodies. *Mineralogical Magazine* 50: 33–39.
- Magalhães, M.C.F., J.D. Pedrosa de Jesus & P.A. Williams, 1988. Phosphate minerals from the Miguel Vaças mine, Alentejo, Portugal. *Journal of the Russell Society* 2: 13–18.
- McLaughlin, D., A.R. Ramsden, J.L. Sharpe & P.A. Williams, 2000. Minerals from the Sandy Flat Pipe, Redbank, Northern Territory. *Australian Journal of Mineralogy* 6: 3–7.
- Newberg, D.W., 1967. Geochemical implications of chrysocollabearing alluvial gravels. *Economic Geology* 62: 932–956.
- Ollier, C., 1984. *Weathering*. Harlow: Longmans.
- Ribbe, P.H., G.V. Gibbs & M.M. Hamil, 1977. A refinement of the structure of diopside, $\text{Cu}_6[\text{Si}_6\text{O}_{18}] \cdot 6\text{H}_2\text{O}$. *American Mineralogist* 62: 807–811.
- Roberts, W.L., T.J. Campbell & G.R. Rapp Jr., 1990. *Encyclopedia of Minerals*. New York: Van Nostrand Reinhold.
- Stumm, W., & J.J. Morgan, 1981. *Aquatic Chemistry*. New York: Wiley and Sons.
- Thompson, W.A., 1980. Chrysocolla pseudomorphs from Ray, Arizona. *Mineralogical Record* 11: 248–250.
- Van Oosterwyck-Gastuche, M.C., 1970. La structure de la chrysocolle. *Comptes Rendus, Académie des Sciences de Paris, Série D* 271: 1837–1840.
- Van Oosterwyck-Gastuche, M.C., & C. Grégoire, 1971. Electron microscopy and diffraction identification of some copper silicates. *Mineralogical Society of Japan Special Paper* 1: 196–205.
- Williams, P.A., 1990. *Oxide Zone Geochemistry*. New York: Ellis Horwood.

Manuscript received 8 November 1999, revised 20 July 2000 and accepted 23 August 2000.

Associate Editor: F.L. Sutherland.